Identification of Suspended Sediment Sources Using Soil Characteristics in a Semiarid Watershed

F. E. Rhoton*
USDA-ARS National Sedimentation Lab.
Oxford, MS 38655

W. E. Emmerich
USDA-ARS Southwest Watershed
  Research Center
Tucson, AZ 85719

D. A. DiCarlo
D. S. McChesney
USDA-ARS National Sedimentation Lab.
Oxford, MS 38655

M. A. Nearing
USDA-ARS Southwest Watershed
  Research Center
Tucson, AZ 85719

J. C. Ritchie
USDA-ARS Hydrology and
  Remote Sensing Lab.
Beltsville, MD 20705

PEDOLOGY

Identification of primary sediment source areas in watersheds is necessary to ensure that best management practices are installed in areas that maximize reductions in sediment and chemical loadings of receiving waters. Our objectives were to use a soil geomorphology–erodibility approach to locate sediment sources in the Walnut Gulch Experimental Watershed (WGEW). Major soil mapping units were sampled along transects in six subwatersheds (SWs). At each sampling point, latitude–longitude, slope gradient, slope aspect, and hillslope position were recorded. Samples collected from the surface 5.0 cm were characterized for a range of basic soil characterization properties. Additionally, ^{137}Cs, ^{40}K, ^{226}Ra, and stable C isotope distributions were quantified as potential source area indicators. Suspended sediment samples collected from WGEW and SW flumes were characterized for the same properties. Relative to the SW soils, the suspended sediments were generally enriched in silt, clay, organic C, inorganic C, total N, extractable cations, extractable Fe and Mn, ^{13}C from C3 plants, ^{40}K, and ^{226}Ra. The suspended sediment from three SWs was enriched in ^{137}Cs. Eleven characterization parameters were used in a multivariate mixing model to identify the SWs contributing the greatest sediment loads in the WGEW. The mixing model results indicated that three SWs were contributing approximately 86% of the sediment, and that the greatest amount originated in the three SWs with the lowest soil aggregation index (highest erodibility). These results were supported by the δ^{13}C data, which indicated that approximately 65% of the stable C isotopes leaving the WGEW during this period were derived from C3 plants (shrubs), the dominant vegetation on the three SWs.

Abbreviations: AI, aggregation index; ER, enrichment ratio; Fe$_d$ and Mn$_d$, citrate–bicarbonate–dithionite extractable Fe and Mn; Fe$_o$ and Mn$_o$, acid ammonium oxalate extractable Fe and Mn; Fe$_p$ and Mn$_p$, sodium pyrophosphate extractable Fe and Mn; OC, organic carbon; SW, subwatershed; WDC, water-dispersible clay; WGEW, Walnut Gulch Experimental Watershed.

The identification of sediment sources in watersheds is important from a number of agricultural and environmental perspectives. Soil losses in the United States have been estimated at 51.5 Mg ha^{-1} yr^{-1} (Pimentel et al., 1995), which results in productivity losses and increased production costs as fertilizer, pesticide, and irrigation application rates must be increased to compensate for erosion losses. The increased use of chemical amendments can further degrade environmental and water quality as offsite accumulation of nutrients and pesticides are enhanced. In 1995, the estimated annual cost for such erosion-induced problems was $37 billion (Pimentel et al., 1995). Given this potential cost, scientific approaches are needed to relate sediment properties back to specific soil conditions in watersheds to better define sediment routing processes, identify source areas of pollutants, and identify needed changes in man-

agement systems to resolve excessive runoff and erosion problems. This is especially important in arid and semiarid regions, where soil erosion can be considered a more serious problem, relative to humid regions, because the soils are generally shallow and less well-developed, with inadequate vegetative cover.

Direct monitoring and fingerprinting are the two primary approaches used in sediment source identification research. Direct monitoring uses technology such as erosion pins, runoff troughs, automated suspended sediment samplers, and manually collected grab samples (Sutherland and Bryan, 1989) to measure sediment yields from potential source areas for determining their relative contribution to overall sediment loads in a watershed. However, since direct monitoring methods cannot be used at scales larger than small drainage basins, they are not useful for distinguishing between source types either within or between individual storm events (Slattery et al., 1995). The other approach, commonly referred to as *fingerprinting*, is best suited for this purpose. Fingerprinting relies on suspended sediment properties for which equivalent values exist in the watershed soils and streambank materials (Slattery et al., 1995). Soil and sediment properties used in this approach include: clay mineralogy, color, chemical composition, radionuclide concentrations, and a range of magnetic susceptibility parameters.

The clay mineralogy of suspended sediment has been used to infer source areas (Neiheisel and Weaver, 1967; Klages and Hsieh, 1975; Wall and Wilding, 1976), but using this approach as a singular method can be problematic because clay minerals are

preferentially eroded from soil surfaces as a function of clay-size distributions (Rhoton et al., 1979) in addition to differential settling of some clay mineral species during transport. The use of sediment color to separate channel and nonchannel sediment sources (Grimshaw and Lewin, 1980) can also lead to erroneous interpretations if there is not sufficient contrast between the color of surface soils and the regolith. Magnetic susceptibility of watershed soils and suspended sediments is used to infer source areas (Oldfield et al., 1979; Slattery et al., 1995; Caitcheon, 1998; Walling, 2005), in particular, topsoil vs. subsoil components (Dearing et al.,1986). Fallout radionuclide (^{7}Be, ^{210}Pb, and ^{137}Cs) ratios are used for fingerprinting suspended sediments in rivers and coastal waters (Walling and Woodward, 1992; Wallbrink et al., 1999; Bonniwell et al., 1999) by differentiating between freshly eroded soil adjacent to streams and collapsed bank material. Peart and Walling (1988) have proposed the use of sediment chemistry as a natural tracer method for determining the origin of suspended sediment. The chemical data, which consist of selective dissolution analyses for Fe, P, C, N, and Mn from soil and suspended sediment samples, are evaluated with a simple mixing model.

Furthermore, soil geomorphology and pedology are important components of sediment source identification due to their influence on soil properties that determine erodibility and sediment characteristics. More specifically, at watershed scales, soil erodibility and sediment characteristics are strongly related to soil properties that determine aggregate stability. The more important soil properties in this regard include clay and organic matter contents, and Fe and Al oxide contents. In general, these properties are strongly influenced by slope factors such as position, shape, aspect, and gradient (Schoeneberger et al., 2002). For example, Franzmeier et al. (1969) reported greater concentrations of organic C on north-facing slopes as a result of lower temperatures and higher soil water contents. In terms of slope position, most studies (Honeycutt et al., 1990; Pierson and Mulla, 1990; Rhoton et al., 2006) have reported greater organic C on footslopes and toeslopes, which account for the greater aggregate stabilities being recorded in these positions. Particle size distributions and basic cations are also distributed as a function of slope position. Young and Hammer (2000) identified higher silt contents and lower basic cation concentrations on backslope positions relative to upslope positions. Similarly, Franzmeier et al. (1969) indicated that particle size distributions were coarser on midslope positions, and basic cations were concentrated on the lower slope positions.

The objective of this research was to use a range of soil and sediment physical, chemical, mineralogical, and radionuclide analyses in conjunction with a multivariate mixing model to identify the primary sources of sediment in a semiarid watershed using a nested watershed arrangement.

MATERIALS AND METHODS
Site Characteristics

The research was conducted on SWs 3, 7, 9, 10, 11, and 15 (Fig. 1) in the WGEW, which encompasses the town of Tombstone, AZ (31°43′ N, 110°41′ W). The watershed contains approximately 150 km^2 in a high foothill alluvial fan portion of the larger San Pedro River watershed at elevations ranging from 1220 to 1950 m. The mean annual temperature is 17.6°C, and the average annual precipitation is 324 mm (Renard et al., 1993), which occurs primarily as high-intensity, short-duration thunderstorms between July and mid-

September (Osborn et al., 1979). Most of the surface runoff occurs during this period (Nichols et al., 2000).

Soil distribution in the WGEW (Fig. 1) is closely related to the composition of the parent material (Rhoton et al., 2007). Specifically, the watershed soils formed on Precambrian to Tertiary-age sandstone, conglomerates, limestone, volcanics, granodiorite, or quartz monzonite (W.R. Osterkamp, unpublished data, 2007). Of these parent materials, Quaternary alluvium from limestone accounts for approximately 80% of the watershed surface (Alonso, 1997). The soils formed on this parent material are well-drained, calcareous gravelly loams (Gelderman, 1970). Those watershed soils formed in alluvium and colluvium from andesite and basalt, and residuum from granodiorite were generally finer textured, shallow, and well drained. Rock and gravel contents at the soil surface can range from 0 to 70% on very steep slopes (Simanton and Toy, 1994). Major vegetation in SWs 3, 7, and 15 consists of the shrub species of creosote bush [*Larrea tridentata* (DC.) Coville], whitethorn (*Acacia constricta* Benth.), tarbush (*Flourensia cernua* DC.), snakeweed [*Gutierrezia sarothrae* (Pursh) Britton & Rusby], and burroweed [*Haplopappus tenuisectus* (Greene) S. F. Blake ex L. D. Benson]. The grass species of black grama [*Bouteloua eriopoda* (Torr.) Torr.], blue grama [*Bouteloua gracilis* (Kunth) Lag. ex Griffiths], side-oats grama [*Bouteloua curtipendula* (Michx.) Torr.], curly-mesquite [*Hilaria belangeri* (Steud.) Nash], and bush muhly (*Muhlenbergia porteri* Scribn. ex Beal) are the dominant vegetation in SWs 9, 10, and 11 (Simanton et al., 1994). The entire watershed is used as rangeland.

Study Approach

All SWs used in the study were instrumented with a supercritical flume (Renard et al., 1993). Suspended sediments were collected with vertical samplers mounted on the face of the flumes. These samples were collected in 30.5-cm increments above the floor of the flume for a total flow depth up to122 cm. During flow events, sediment entered through 6.4-mm-diameter ports drilled into the 10.2-cm-diameter (i.d.) aluminum tube used for the samplers. Plastic tubing connected the ports to 500-mL plastic sample bottles mounted inside the sealed sampler at each depth. Additionally, 2-L sample bottles were attached to the bottom of the samplers to ensure that sufficient volumes of sediment were obtained at the 30.5-cm flow depth during low-flow events. Once filled, float valves sealed the sample bottles to prevent continuous flow-through of suspended sediments for a more accurate estimate of sediment concentrations. Suspended samples collected between 1999 and 2003 were analyzed by year. These yearly data were then averaged to give one overall value per flume.

Soil samples were collected from the SWs based on relative acreage occupied by individual mapping units. This involved superimposing the digitized soil survey (1:5000) on the digital elevation model (DEM) for each SW. A sampling transect length of 1000 m was arbitrarily chosen for each 200 ha of a given soil mapping unit (Fig. 2). The transects were delineated on the DEM using geographic positioning system derived coordinates such that a range of surface morphometry factors (Schoeneberger et al., 2002) were represented by the samples. Specifically, soil samples were collected with respect to slope position, class, and aspect. At each selected location, samples were obtained from the surface 5.0 cm at three points, approximately 10 m apart and perpendicular to the slope, composited, and sealed in a plastic bag. This sampling depth generally represents the A horizon thickness according to Breckenfeld et al. (1995), and that fraction of the profile most affected by erosion processes involving rill formation
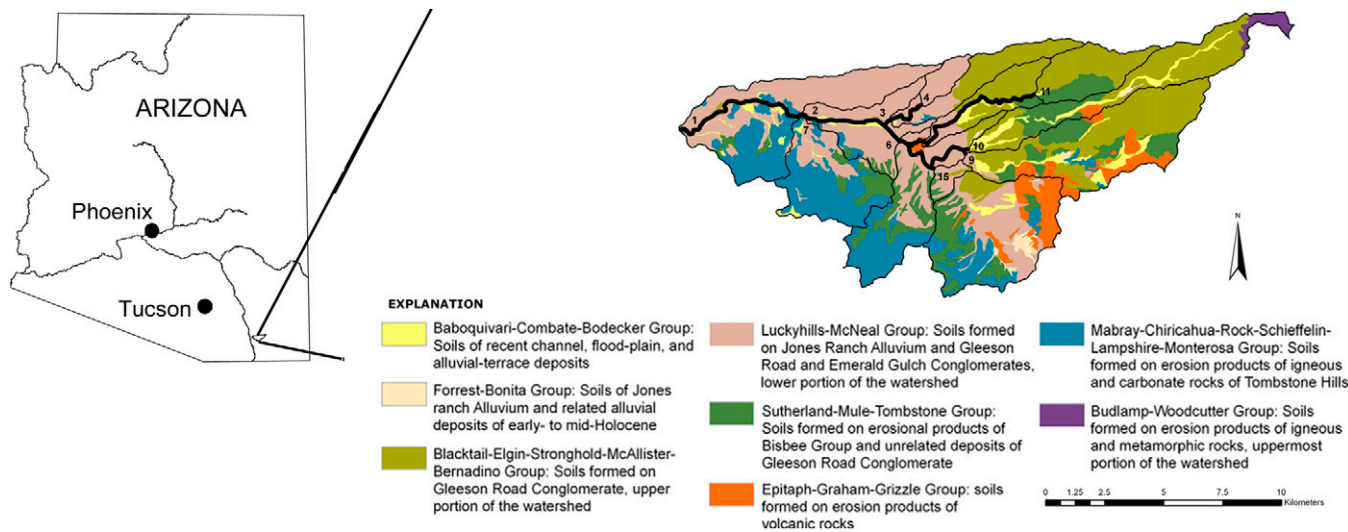
Fig. 1. Location of various subwatersheds in the Walnut Gulch Experimental Watershed, Arizona.

and infilling. Thus, the data probably include contributions from both A and upper B horizons in various proportions. Site data were recorded for latitude–longitude, slope position, slope steepness, and slope aspect.

Laboratory Analyses

In the laboratory, all soil and sediment samples were air-dried or oven-dried at 60°C and sieved to <2 mm. Particle size distribution was determined by standard pipette analysis following overnight dispersion in Na hexametaphosphate (NRCS, 1996). The water-dispersible clay (WDC) component of the total clay fraction was also estimated by this methodology, using only distilled water as the dispersant. The total clay and WDC content data were used to calculate an aggregation index (AI) for the watershed soils based on the method of Harris (1971) as follows: AI = 100 (1 – WDC/total clay). Soil pH was measured in a 1:1 soil/distilled water (v/v) suspen-

sion (McLean, 1982). Total C and N were determined by combusting 0.5-g samples in a LECO CN-2000 CN analyzer (LECO Corp., St. Joseph, MI). The inorganic fraction of the total C was quantified by treating a separate 1-g sample with 5 mol L^{-1} HCl in a sealed decomposition vessel (200 mL) fitted with a rubber septum. Carbon dioxide pressure generated by the acid decomposition of the sample was measured with a tensimeter (Soil Measurement Systems, Tucson, AZ) probe inserted through the septum. Pressure readings were then converted to C contents using a standard curve, and subtracted from total C to give the organic C (OC) content (Rhoton et al., 2006). The sodium pyrophosphate (p), acid ammonium oxalate (o), and sodium citrate–bicarbonate–dithionite (d) extractable Fe and Mn contents, in addition to NH4OAc-exchangeable cations of the soils and sediment, were determined by the procedures of the NRCS (1996). All extracts were analyzed by atomic absorption spectrophotometry.

Radionuclide (^{137}Cs, ^{40}K, and ^{226}Ra) activities were measured simultaneously by gamma spectroscopy using <2-mm materials and the methods of Whiting et al. (2005). The K and Ra isotopes were included since they represent natural sources whose concentrations can vary considerably depending on the source material. The $\delta^{13}C$ was determined by the Stable Isotope Lab at the University of California-Davis using a PDZ Europa mass spectrometer (Northwich, UK). As a pretreatment for stable C isotope analysis, carbonate C was removed by shaking all samples in a 10% acetic acid solution until effervescence ceased. The samples were then washed three times in distilled water and centrifuged after each washing. Procedural details were identical to those reported elsewhere (Biedenbender et al., 2004; Bekele and Hudnall, 2003). The relative contributions of C3 and C4 plants

Mapping Units

- Combate
- Epitaph
- Forrest-Bonita
- Graham
- Graham-Lampshire complex
- Grizzle
- Luckyhills-McNeal complex
- Mabray-Chiricahua-Rock outcrop complex
- Mabray-Rock outcrop
- McAllister-Stronghold complex
- Monterosa
- Sutherland
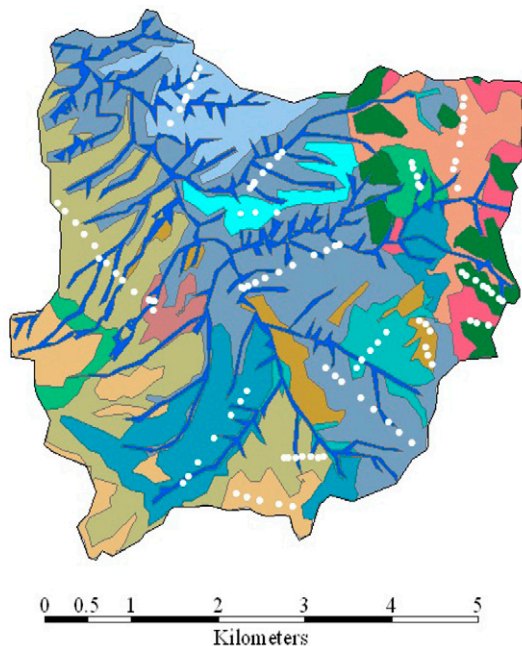- Tombstone
- Sampling points along transects

Fig. 2. Watershed sampling approach based on relative area of sampling units, showing sampling points along transects in Subwatershed 15.

to δ^{13}C were estimated by the mass balance equation of Boutton (1996) as follows:

$$x = \delta^{13}C_{soil,\ sediment} - \delta^{13}C_{C3} / \delta^{13}C_{C4} - \delta^{13}C_{C3}$$

where x is the relative amount of C derived from C4 plants, $\delta^{13}C_{soil,\ sediment}$ is the δ^{13}C of the soil and sediment organic fractions, $\delta^{13}C_{C4}$ is the average δ^{13}C value of the C4 plants (–13‰), and $\delta^{13}CC3$ is the average δ^{13}C value of C3 plants (–27‰). The relative amount of C derived from C3 plants is $1 - x$.

Quantitative soil color was measured with a Minolta Chroma Meter (Minolta Corp., Ramsey, NJ). Magnetic susceptibility (MS) was determined with a Bartington MS-2 magnetic susceptibility meter (Bartington Instruments, Oxford, UK). The mineralogy of the soil and sediment clay fractions ($<$2 μm) was determined with a Philips APD 3520 x-ray diffraction unit (Philips Electronic Instruments, Mahwah, NJ) using Cu Kα radiation (35 kV, 20 mA). Clay specimens were step-scanned between 2 and 32° 2θ at 0.075° 2θ increments with a counting time of 5 s per increment. The treatments consisted of scanning a K-saturated specimen in an air-dry state and then heating to 300 and 550°C for 2 h. A separate specimen was scanned following Mg saturation and glycerol solvation. All statistical analysis related to soil and sediment properties used the GLM and CORR procedures of SAS Version 8 (SAS Institute, 1999).

The relative contribution of each SW to the sediment load leaving the WGEW at Flume 1 was estimated using a multivariate mixing model method in conjunction with signatures for the suspended sediment physical and chemical characterization parameters. This was accomplished by the following linear optimization procedure. Each suspended sediment property was normalized by its mean, and these properties were placed into a sediment property vector, $\mathbf{d}_i$, where the subscript i refers to the SW from which the sample was taken for each flume (SW). The linear optimization problem becomes finding the vector ($\mathbf{x}$) containing the proportion of sediment from each SW that minimizes the function $(\mathbf{Cx} - \mathbf{d})'(\mathbf{Cx} - \mathbf{d}) = 0$, where $\mathbf{C}$ is the matrix made up of the sediment property vectors of the contributing SWs and $\mathbf{d}$ is the sediment property vector of the outlet watershed. This routine was run and the physical and chemical signature of the sediment at Flume 1 was expressed in terms of possible contributions from Flumes 3, 7, 9, 10, 11, and 15. The average measurements of the characterization parameters in each SW can be directly input into the mixing model.

While this gives an estimate of individual SW contributions, it only uses the means of the measurements; it does not take into account the distribution of the data. To accommodate the known distribution in the measured data and to obtain an estimate of how the uncertainties propagate through the mixing model, a Monte Carlo routine was added to the mixing model similar to that reported in previous studies (Heimsath et al., 2002; Dibben et al., 1998; Bekesi and McConchie, 1999; Faulkner et al., 2003). Briefly, the mean and the standard deviation of the mean were obtained from the distribution of each suspended sediment parameter within a SW. Random values were then chosen for each parameter using a Gaussian distribution and the measured means and standard deviations for that SW. The randomly chosen data were run through the mixing model and the results tabulated. This process was repeated 10,000 times, which gives an estimate of the means and distribution of individual SW contributions to the sediment load at Flume 1.

RESULTS AND DISCUSSION
Watershed Soil vs. Sediment Characteristics

The soil mapping units and associated landforms in the WGEW are provided in Table 1. Most of the soils in the watershed were developed on a fan remnant landform (Breckenfeld et al., 1995). In terms of the entire watershed, the Luckyhills–McNeal complex very gravelly sandy loam is most extensive, occupying approximately 4300 ha (Table 2). Other mapping units comprising substantial acreages are the Elgin–Stronghold complex very gravelly fine sandy loam (1509 ha), McAllister–Stronghold complex gravelly fine sandy loam (1363 ha), and Tombstone extremely gravelly sandy loam (1280 ha).

Selected physical and chemical properties of the soils and corresponding sediment are shown as averages by individual SW (Tables 3 and 4). The distribution of some properties seemingly reflect differences in parent material composition between SWs. For example, SWs 3 and 7 are considerably different from the other SWs in terms of total clay, OC, AI, magnetic susceptibility, and hue. In SW 7, approximately 60% of the soils were formed on igneous residuum (i.e., granite and granodiorite) compared with limestone, andesite, and basalt parent materials in the other SWs. Consequently, soils in SW 7 have lower clay and OC contents that translate into a lower AI because less weathering and soil development has occurred on these parent materials. The igneous parent materials in SW 7 also account for the highest soil magnetic susceptibility readings, as igneous rocks generally contain higher magnetite contents. The higher Munsell color readings in SW 7 soils are attributed to lighter colored, high quartz content, granitic rocks and lower OC contents. The calcareous, alluvium parent materials in SW 3 also resulted in lighter colored soils, a high pH, relatively low clay and OC contents, and the lowest recorded AI for the watershed. By contrast, SW 9 contained substantial areas of soils formed from fine-grained igneous parent materials (i.e., andesite and basalt), which produce soils with finer particle sizes. These soils had the highest total clay contents and AI, and associated low average hue and value readings. Apparently, parent material has a substantial impact on the physical and chemical behavior of soils in the WGEW.

The physical properties of the suspended sediments (Table 3) indicate that the particle size distributions of suspended sediments were finer than the soils within the SWs due to particle size selectivity created by soil erosion and sediment transport processes. The ratios determined for suspended sediment vs. watershed soil properties indicate that, relative to the watershed soils, clay contents of the sediment were enriched by an average factor of 1.31. The greatest enrichment occurred in SWs 7 (1.59) and 3 (1.55). These two SWs had the lowest values for AI (Table 3). The sediment from SW 9 was depleted in clay (0.93) relative to its soils. This indicates that, overall, SWs 7 and 3 had the most highly erodible soils in the WGEW and SW 9 had the least erodible. These enrichment ratios (ER) of suspended sediment clays/soil clays were correlated against the SW soil AI for the six individual SWs. The resulting correlation coefficient (r) was –0.946 ($P \leq 0.01$), a clear indication that AI can be used to assess the erodibility of these soils. Furthermore, suspended sediments were more enriched in silt-size material

Table 1. Soil taxonomy and landforms of mapping units in Walnut Gulch Experimental Watershed.

Soil phase	Taxonomic classification	Landform
Baboquivari gravelly coarse sandy loam	fine-loamy, mixed, thermic Ustic Haplargids	fan remnant
Bernardino gravelly clay loam	fine, mixed, superactive, thermic Ustic Calciargids	fan remnant
Blacktail gravelly sandy loam	fine, mixed, superactive, Calcidic Agriustolls	fan remnant
Bodecker extremely gravelly sandy loam	sandy-skeletal, mixed, thermic Ustic Torriorthents	flood plains
Bonita cobbly silty clay	fine, smectitic, thermic Typic Haplotorrerts	flood plains
Budlamp very gravelly fine sandy loam	loamy-skeletal, mixed, thermic Lithic Haplustolls	mountains
Chiricahua very cobbly loam	clayey, mixed, superactive, thermic, shallow Ustic Haplargids	hills
Combate gravelly loamy coarse sand	coarse-loamy, mixed, non-acid, thermic Ustic Torrifluvents	alluvial fans
Elgin very gravelly fine sandy loam	fine, mixed, thermic Calcic Paleargids	fan remnant
Epitaph very cobbly clay loam	fine, smectitic, thermic Petrocalcic Calcitorrerts	hills
Forrest loam	fine, mixed, superactive, thermic Ustic Calciargids	basin floor
Graham cobbly clay loam	clayey, smectitic, thermic Lithic Ustic Haplargids	hills
Grizzle coarse sandy loam	fine loamy, mixed, superactive, thermic Ustic Calciargids	hills
Lampshire very cobbly loam	loamy-skeletal, mixed, superactive, non-acid, thermic Lithic Ustic Torriorthents	hills
Luckyhills very gravelly sandy loam	coarse-loamy, mixed, thermic Ustic Haplocalcids	fan remnant
McAllister loam	fine-loamy, mixed, thermic Ustic Calciargids	fan remnant
McNeal gravelly sandy loam	fine-loamy, mixed, thermic Ustic Calciargids	fan remnant
Mabray very gravelly loam	loamy-skeletal, carbonatic, thermic Lithic Ustic Torriorthents	hills
Monterosa very gravelly sandy loam	loamy-skeletal, mixed, superactive, thermic, shallow Ustic Petrocalcids	fan remnant
Mule very gravelly fine sandy loam	loamy-skeletal, carbonatic, thermic Ustic Haplocalcids	fan remnant
Schiefflin very stony loamy sand	mixed, thermic Lithic Torripsamments	hills
Stronghold gravelly fine sandy loam	coarse-loamy, mixed, thermic Ustic Haplocalcids	fan remnant
Sutherland gravelly fine sandy loam	loamy-skeletal, carbonatic, thermic, shallow Calcic Petrocalcids	fan remnant
Tombstone extremely gravelly fine sandy loam	loamy-skeletal, mixed, thermic Ustic Haplocalcids	fan remnant
Woodcutter very gravelly fine sandy loam	loamy-skeletal, mixed, thermic Lithic Agriustolls	hills and mountains

relative to the clay fractions in most SWs by a factor of two to three times.

Based on the highest ER for clay and the lowest soil AI (Table 3), both indicators of low aggregate stability and high erodibility, SW 3 would be expected to produce the greatest amounts of sediment in the runoff on a per-unit-area basis for a given rainfall event. Following SW 3, the order for clay ER is 7 > 15 > 11 > 10 > 9. The order for AI by SW is 9 > 15 ≥ 10 > 11 > 7 > 3. These results may be substantiated by the average suspended sediment concentrations measured at each of the flumes, which are reasonably close to expected results based on the ER and AI. Obviously, the relative land areas associated with the various slope factor components in each SW also have a strong influence on sediment yields measured at each flume, but the use of soil–sediment factors such as ER and AI appears to be a reasonable approach to estimating potential sediment yields in the SWs.

In terms of color, the Munsell notations for the suspended sediments were generally higher than the watershed soils, which may be due to the large silt enrichment of the sediments relative to the soils.

Magnetic susceptibility of the sediments ranged from 104 (SW 3) to 226×10^{-8} m^3 kg^{-1} (SW 7). The magnetic susceptibility ratios for suspended sediments vs. SW soils averaged 0.56, indicating that the suspended sediments were depleted relative to the soils. This suggests that the soil magnetic fraction, primarily magnetite, is concentrated in the sand-size fraction, which is also depleted in the suspended sediment. Since magnetic susceptibility is so particle size dependent, an accurate assessment of this soil property as a fingerprinting tool requires that similar particle size distributions be used when measuring soil and sediment samples.

Soil organic C (Table 4) varied significantly ($P \leq 0.05$) between SWs. For example, SW 15 contained nearly twice the concentration of SW 7 soils. Organic C contents of the suspended sediments averaged 24.3 g kg^{-1}, compared with 11.4 g kg^{-1} for the watershed soils. Thus, the OC contents of the suspended sediments were enriched by an average ratio of 2.13 relative to watershed soils. The highest OC concentrations in the suspended sediments were associated with the lower AI soils, especially SWs 3 and 7. Total soil N contents were closely related to OC contents, which accounts for SW 15 having significantly ($P \leq 0.05$) greater amounts than the other SWs. The C/N ratios exhibited more mean separation between SWs than the OC and N components taken individually. Total N content of the suspended sediment was statistically similar between SWs and was approximately 6% of the OC contents, with C/N ratios slightly higher in the sediments.

There were some significant differences in pH between SWs, which ranged from 8.6 to 6.9 (Table 4). The higher pH values are attributed to greater CaCO$_3$ concentrations in SWs 3 and 11. The lower readings for soils in SWs 9 and 10 may be the result of higher acid clay contents. Suspended sediment pH averaged slightly lower than the soils, possibly the result of the much higher OC contents in the sediment. Calcium was the dominant extractable cation in the watershed soils, with concentrations ranging from 2678 to 6371 mg kg^{-1}. No statistically significant differences were found between SWs with the exception of SW 10, which had significantly lower concentrations due to a large area of soils formed on noncarbonatic parent materials. The distribution of Mg, K, and Na was

fairly uniform between the SWs, with the highest concentrations identified in SWs 9, 10, and 15, where most of the basalt- and andesite-derived soils exist. Suspended sediments were enriched in all extractable cations relative to the soils. The average ratios were Ca, 1.39; Mg, 1.31; K, 1.26; and Na, 1.61. These results are consistent with the clay, silt, and inorganic C enrichment of the sediment. Extractable Fe and Mn contents were generally low and not significantly different between SWs with the exception of Fe_d, which was significantly greater in SWs 7 and 10. The extractable Fe data for suspended sediments were substantially higher than the data for the soils for all three extractants in all SWs. The higher Fe_p values may be explained by the higher OC contents in the sediment, while the increases in Fe_o and Fe_d can be largely attributed to the enhanced silt and clay contents of the sediment. Both of these soil components are transported as clay coatings or as discrete particles. The extractable Mn component showed consistent increases only in the suspended sediment phase for the Mn_d phase, and there were basically no differences between SWs.

Table 2. Mapping unit areas for the subwatersheds (SWs) studied in the Walnut Gulch Experimental Watershed.

Soil mapping unit	Area					
	SW 3	SW 7	SW 9	SW 10	SW 11	SW 15
	ha					
Baboquivari–Combate complex		19.5	188.7	190.1	6.7	
Blacktail gravelly sandy loam				245.5		
Budlamp–Woodcutter complex				64.6		
Chiricahua very gravelly clay loam		101.3				
Combate loamy sand	3.0	8.2				60.0
Elgin–Stronghold complex	120.2		881.7	283.7	75.3	
Epitaph very cobbly loam			71.9	18.1		152.7
Forrest–Bonita complex			12.6	18.7		103.2
Graham cobbly clay loam			175.7	13.8		66.8
Graham-Lampshire complex			122.1	9.1		113.4
Grizzle coarse sandy loam						81.6
Lampshire–rock outcrop complex		28.4	52.5			
Luckyhills loamy sand		14.0	7.0			
Luckyhills–McNeal complex	443.4	286.8	44.6	1.1		740.1
Mabray–Chiricahua–rock outcrop complex		295.8				36.3
Mabray–rock outcrop complex		193.4				150.7
McAllister–Stronghold complex	273.0		317.4	229.3	61.4	144.8
Monterosa very gravelly fine sandy loam	12.7	15.6				248.6
Riverwash–Bodecker complex		8.1		12.6		
Schiefflin very stony loamy sand		190.2				
Stronghold–Bernadino complex	94.9		38.6	178.8	421.1	
Sutherland–Mule complex		65.7				
Sutherland very gravelly fine sandy loam		141.2				403.9
Tombstone very gravelly fine sandy loam			486.3	252.0	223.6	73.4
Woodcutter gravelly sandy loam				61.9		
Totals	947.2	1368.1	2398.9	1579.4	788.2	2375.6

The stable C isotope data for the soils (Table 5) indicate that the organic C fraction ranged from –17.70‰ (SW 11) to –20.90‰ (SW 7), and averaged –18.95‰, which is near the intermediate point of mean $\delta^{13}C$ values reported for C3 (–27‰) and C4 (–13‰) plants by several researchers (Ambrose and Sikes, 1991; McPherson et al., 1993; Boutton et al., 1998). In this regard, SWs 3 (–19.52‰), 7 (–20.90‰), and 15 (–19.23‰) had the lowest values, suggesting that the OC fractions in these soils contain greater contributions from C3 plants (trees and shrubs) relative to C4 plants (grasses). The mean $\delta^{13}C$ data for the suspended sediment (Table 5) had consistently lower values, which averaged –21.49 vs. –18.95‰ for the soils. Apparently, the sediment is enriched in OC of C3

plant origin relative to C4 plants, or C3-derived C is being preferentially eroded from these watershed soils. This is verified by the calculations for the relative contributions of C3 and C4 to $\delta^{13}C$ for the OC fraction. These data show that the OC in the soil was predominantly of C4 plant origin, with the exception of SW 7. Conversely, an opposite trend exists for the sediment, where the OC of C3 plant origins predominates, especially in SWs 3 and 7 and at Flume 1. These data strongly suggest that the OC from the C3 plants is being preferentially eroded from the soils and transported through the WGEW.

The distribution of radionuclides in the watershed soils (Table 6) indicates that the ^{137}CS concentrations ranged from 11.1 (SW 11) to 16.5 Bq kg^{-1} (SW 10) and averaged

Table 3. Selected physical properties of soils and suspended sediments for individual subwatersheds (SWs).

Property†	SW 1		SW 3		SW 7		SW 9		SW 10		SW 11		SW 15	
	Soil	Sediment	Soil	Sediment	Soil	Sediment	Soil	Sediment	Soil	Sediment	Soil	Sediment	Soil	Sediment
Sand, g kg^{-1}	–	333 ab‡	720 a	375 ab	719 a	477 ab	653 b	428 ab	698 a	379 ab	731 a	467 a	608 c	433 ab
Silt, g kg^{-1}	–	432 a	148 c	413 a	162 bc	335 a	184 b	421 a	142 c	443 a	136 c	348 a	251 a	387 a
Clay, g kg^{-1}	–	235 ab	133 bc	212 ab	118 c	188 ab	163 a	151 b	160 a	178 ab	133 bc	185 ab	141 b	180 ab
WDC, g kg^{-1}	–	–	108 ab	–	91 c	–	111 ab	–	116 a	–	102 bc	–	98 bc	–
AI	–	–	18.0 c	–	22.8 c	–	31.9 a	–	28.1 b	–	23.9 c	–	28.2 b	–
MS, 10^{-8} m^3 kg^{-1}	–	157 b	198 b	104 d	800 a	226 a	294 b	170 b	189 b	124 cd	264 b	158 b	217 b	115 cd
Hue§	–	7.4 b	7.1 b	6.7 c	8.2 a	8.6 a	6.5 d	6.9 c	6.4 d	6.6 c	6.8 c	7.1 bc	6.9 bc	6.8 c
Value	–	3.4 a	3.1 ab	3.5 ab	3.3 a	3.5 ab	2.9 c	3.4 ab	3.0 c	3.3 b	3.1 b	3.6 a	3.1 b	3.5 ab
Chroma	–	2.0 b	2.0 ab	2.1 a	2.0 a	2.0 b	1.7 c	1.8 c	1.8 c	1.9 bc	1.5 d	1.8 c	1.8 bc	1.9 bc

† WDC, water-dispersible clay; AI, aggregation index; MS, magnetic susceptibility.

‡ Values followed by the same letter are not statistically different at $P \leq 0.05$ based on Duncan's multiple range test.

§ All hues are yellow red (YR).

Table 4. Selected chemical properties of soils and suspended sediments for individual subwatersheds (SWs).

Property†	SW 1 Soil	SW 1 Sediment	SW 3 Soil	SW 3 Sediment	SW 7 Soil	SW 7 Sediment	SW 9 Soil	SW 9 Sediment	SW 10 Soil	SW 10 Sediment	SW 11 Soil	SW 11 Sediment	SW 15 Soil	SW 15 Sediment
Organic C, g kg⁻¹	–	25.6 ab‡	10.2 bc	29.9 a	8.5 c	26.5 ab	12.1 ab	19.9 b	11.5 b	20.0 b	11.8 b	23.6 b	14.2 a	26.1 ab
Inorganic C, g kg⁻¹	–	17.2 c	12.5 ab	18.2 bc	10.1 bc	19.0 bc	7.2 cd	11.0 d	4.9 d	8.8 d	15.0 a	25.3 a	15.0 a	21.8 ab
Total N, g kg⁻¹	–	1.69 ab	0.62 b	1.76 a	0.62 b	1.75 ab	0.76 b	1.26 b	0.74 b	1.28 ab	0.64 b	1.38 ab	0.99 a	1.56 ab
C/N	–	16.2 b	17.4 b	17.7 ab	13.7 c	15.8 b	16.8 b	16.7 a	17.6 b	16.5 b	19.1 a	17.5 a	15.4 c	17.3 ab
pH	–	7.6 ab	8.6 a	7.8 ab	7.9 b	7.6 ab	7.4 c	7.6 ab	6.9 d	7.6 ab	8.5 a	7.8 ab	7.9 b	7.8 ab
Extractable Ca, mg kg⁻¹	–	7349 a	6370 a	7464 a	5521 a	7296 a	5462 a	7546 a	2678 b	6990 a	6371 a	7832 a	5985 a	7740 a
Extractable Mg, mg kg⁻¹	–	272 a	126 b	249 a	142 ab	242 a	268 a	254 a	224 a	232 a	124 b	219 a	189 ab	206 a
Extractable K, mg kg⁻¹	–	450 a	296 a	461 a	272 a	394 a	563 a	576 a	341 a	424 a	274 a	383 a	445 a	528 a
Extractable Na, mg kg⁻¹	–	22.1 a	9.5 a	14.3 a	9.3 a	19.5 a	21.7 a	24.1 a	14.7 a	19.8 a	7.0 a	15.8 a	8.4 a	21.3 a
Fe$_p$, g kg⁻¹	–	0.11 ab	0.02 b	0.11 ab	0.03 b	0.10 ab	0.08 ab	0.09 bc	0.14 a	0.14 a	0.01 b	0.04 d	0.05 b	0.06 cd
Fe$_o$, g kg⁻¹	–	0.91 b	0.20 a	0.71 b	0.71 a	1.89 a	0.27 a	0.48 b	0.40 a	0.72 b	0.15 a	0.34 b	0.28 a	0.51 b
Fe$_d$, g kg⁻¹	–	5.38 abcd	3.76 c	5.60 abc	5.46 ab	6.47 a	4.42 bc	4.77 cd	5.34 a	6.11 ab	3.43 c	4.14 d	3.91 c	4.99 bcd
Mn$_p$, g kg⁻¹	–	0.04 c	0.03 b	0.03 c	0.03 b	0.04 c	0.06 ab	0.08 b	0.10 a	0.13 a	0.03 b	0.03 c	0.04 ab	0.03 c
Mn$_o$, g kg⁻¹	–	0.18 b	0.16 b	0.16 b	0.32 a	0.30 a	0.23 ab	0.22 ab	0.24 ab	0.27 a	0.20 b	0.15 b	0.16 b	0.16 b
Mn$_d$, g kg⁻¹	–	0.35 b	0.19 b	0.32 b	0.40 a	0.52 a	0.26 a	0.33 b	0.26 ab	0.41 ab	0.23 b	0.41 b	0.24 b	0.34 b

† Subscripts p, o, and d denote pyrophosphate-, oxalate-, and dithionite-extractable, respectively.

‡ Values followed by the same letter are not statistically different at $P \leq 0.05$ based on Duncan's multiple range test.

13.1 Bq kg⁻¹. The ^{137}Cs concentrations are apparently controlled by the soil clay contents. Specifically, the highest concentrations were found in SWs 9 and 10, whose soils also contained significantly greater clay contents than those of other SWs. This is consistent with literature reviews (Ritchie and McHenry,1990), which indicate that ^{137}Cs is rapidly and strongly adsorbed in essentially a nonexchangeable form by the clay and organic matter fractions in soils, and that the concentrations decrease exponentially with depth (Ritchie et al., 1970, 1972). The ^{137}Cs activities in the suspended sediments were low relative to the soils. This was unexpected considering the high clay enrichment in the sediment and the strong relationship between ^{137}Cs and soil clays. This suggests that some clay source areas such as rills, gullies, and stream channels are depleted in ^{137}Cs relative to clays eroded from soil surfaces.

The [40]K activities ranged from 515 (SW 15) to 737 Bq kg⁻¹ (SW 10) and averaged 591 Bq kg⁻¹. The reason for this wide range is unclear except that the highest concentration, as for Cs, occurred in SW 10, which had the second highest clay content; but SW 9, with similar clay contents, had considerably lower [40]K concentrations. Furthermore, SW 3 had a high [40]K activity with a low clay content. This may be due to differences in clay mineralogy among watershed soils and parent material. Previous studies (Wilson et al., 2005) have shown that [40]K contents of igneous rocks are much greater than sedimentary rocks, and that granitic rocks average three times greater than basalt (>1000 vs. 300 Bq kg⁻¹). Other scientists (Ibrahim et al., 1993) have reported average [40]K concentrations of 345 Bq kg⁻¹ in finer textured soils and an average of 186 Bq kg⁻¹ in sandy soils. Suspended sediment concentrations of [40]K averaged 1321 Bq kg⁻¹ at the six flumes, indicating that the sediment was enriched by a factor of 2.24 relative to the soils. The highest concentrations were recorded for SWs 3 and 10, which also had the highest soil [40]K concentrations.

The [226]Ra concentrations in the watershed soils ranged from 25.4 to 39.7 Bq kg⁻¹, with an average of 32.0 Bq kg⁻¹. The two highest concentrations occurred in SWs 10 and 3, similar to the [40]K distributions. In this regard, [226]Ra distributions are similar to [40]K in that the higher concentrations are associated with clay soils (Christensen et al., 1990). The [226]Ra contents of the suspended sediment were also greatest at SWs 10 (101.7 Bq kg⁻¹) and 3 (87.7 Bq kg⁻¹). The average for the six flumes was 73.5 Bq kg⁻¹, which is 2.3 times greater than that of the watershed soils.

The clay mineralogy of selected soil mapping units and suspended sediment for SWs 3, 7, and 15 is shown in Fig. 3 to 5. The soils selected represent the greatest areas in these three SWs, which, based on mixing model calculations, contribute approximately 86% of the sediment leaving the WGEW. These mixing model results will be discussed in detail below. The x-ray diffraction patterns from SW 3 (Fig. 3) indicate that the clay mineralogy of the watershed soils is predominantly

Table 5. Average δ^{13}C values for soils and suspended sediments and their partitioning between C3 and C4 plants.

Subwatershed or flume	δ^{13}C Soil	δ^{13}C Sediment	Contribution to organic δ^{13}C — Soil C3	Soil C4	Sediment C3	Sediment C4
	‰	‰	%	%	%	%
1	–	−22.15	–	–	63.8	36.2
3	−19.52	−22.72	44.5	55.5	68.1	31.9
7	−20.90	−23.03	54.2	45.8	65.7	34.3
9	−18.09	−20.51	34.3	65.7	51.9	48.1
10	−18.24	−20.58	35.5	64.5	51.3	48.7
11	−17.70	−20.76	31.7	68.3	55.7	44.3
15	−19.23	−21.31	42.4	57.6	55.3	44.7

Table 6. Average ^{137}Cs, [40]K, and [226]Ra values for soils and suspended sediments.

Subwatershed or flume	[137]Cs Soil	[137]Cs Sediment	[40]K Soil	[40]K Sediment	[226]Ra Soil	[226]Ra Sediment
	Bq kg⁻¹					
1	–	13.6	–	1098	–	85.1
3	11.2	9.1	620	1444	38.9	87.7
7	12.8	14.2	592	1239	25.7	75.8
9	14.2	10.5	581	1306	27.7	27.3
10	16.5	7.0	737	1532	39.7	101.7
11	11.1	12.7	498	1234	34.8	76.6
15	12.8	18.5	515	1171	25.4	71.8

vermiculite (1.43 nm), chloritized vermiculite (1.43–1.77 nm), and smectite (1.77 nm) in that order, with lesser amounts of illite, kaolinite, and quartz. The mineralogy of the suspended sediment clays leaving this SW contains a higher content of smectite, which suggests that this mineral is being preferentially transported from the watershed. This is probably due to the fact that smectite is most concentrated in the fine clay fractions (<0.2 μm) of most soils. In SW 7 (Fig. 4), these smectite, chloritized vermiculite, and vermiculite minerals still predominate, but the composition has shifted more toward the smectite component. This is especially true for the Schiefflin soil, but the 1.77-nm peak areas for the other three soils are broader and not so clearly defined, indicating a lower degree of crystallinity. Another difference is the apparent slight increase in crystallinity but diminished area of the vermiculite component at 1.43 nm. The suspended sediment clay mineralogy x-ray diffraction pattern very closely mirrors that of the Schiefflin soil. More specifically, it is dominated by an intense, well-crystallized smectite component, again indicating that smectite is being preferentially eroded from the soils in the WGEW. The clay mineralogy of the SW 15 soils (Fig. 5) is considerably different from the other two SWs. The vermiculite and expandable (smectite) minerals are the primary components but the peaks are broader, less well-defined, and much less intense, with the exception of the Epitaph soil, which has a prominent expandable smectite peak. The sediment mineralogy from this SW most closely resembles that of the Luckyhills–McNeal complex, which occupies approximately 31% of the SW. A comparison of the watershed soil clay x-ray diffraction patterns with that of the suspended sediment clay leaving the watershed at Flume 1 (Fig. 6) indicates that all of the suspended sediment clays are smectite rich with the exception of SW 15, and that the most intense smectite peaks (1.77 nm) occur at Flumes 9 and 11.

Sediment Source Estimations

Eleven of the 26 suspended sediment characterization properties (Tables 3–6) were selected for use in the mixing model to determine the relative contribution of each SW to the suspended sediment load leaving the watershed at Flume 1. These properties i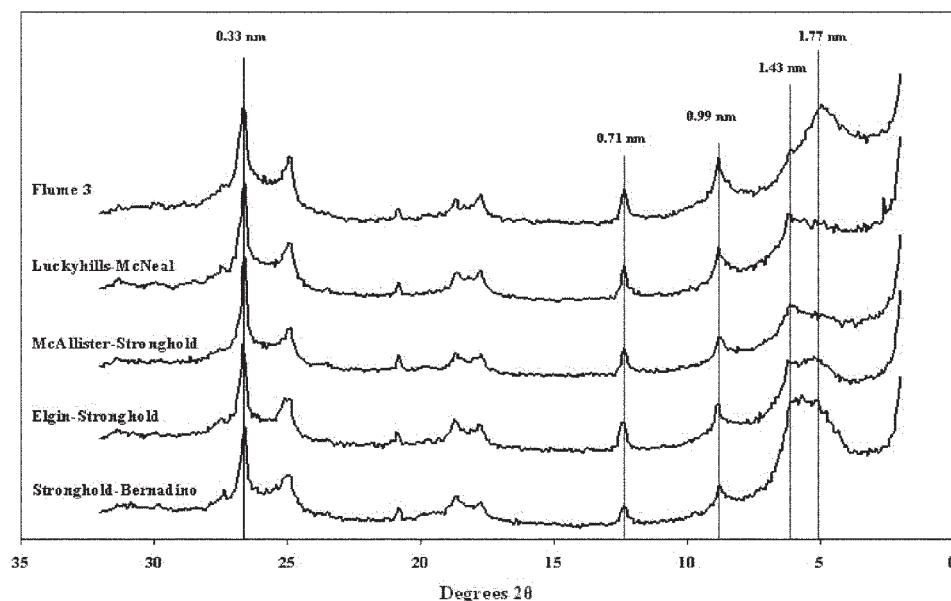ncluded magnetic susceptibility, total N, inorganic C, Fe_d, Mn_d, Fe_o, Mn_o, Fe_p, Mn_p, ^{137}Cs, and [226]Ra. The criteria used for selecting these properties included: a relatively wide range in the normalized values between SWs; minimal evidence of enrichment during the runoff process at the SW flume; and the sediment property value measured at Flume 1 had to be within the range measured at the SW flumes. Also, sediment properties such as pH and those calculated from ratios were not used in the mixing model. No attempt was made to use the clay mineralogy results due to the semiquantitative nature of the analyses. Additionally, the six SWs monitored in this study encompassed approximately 65% of the area in the WGEW. The only unsampled areas were three SWs (1, 2, and 6) on the main channel. Since the sediment load at these three flumes included contributions from the six upstream SWs, no attempt was made to use the data other than that collected at

Fig. 3. Mineralogy of Mg-saturated, glycerol-solvated clays (<2 μm) from suspended sediments and selected watershed soils for Subwatershed 3.
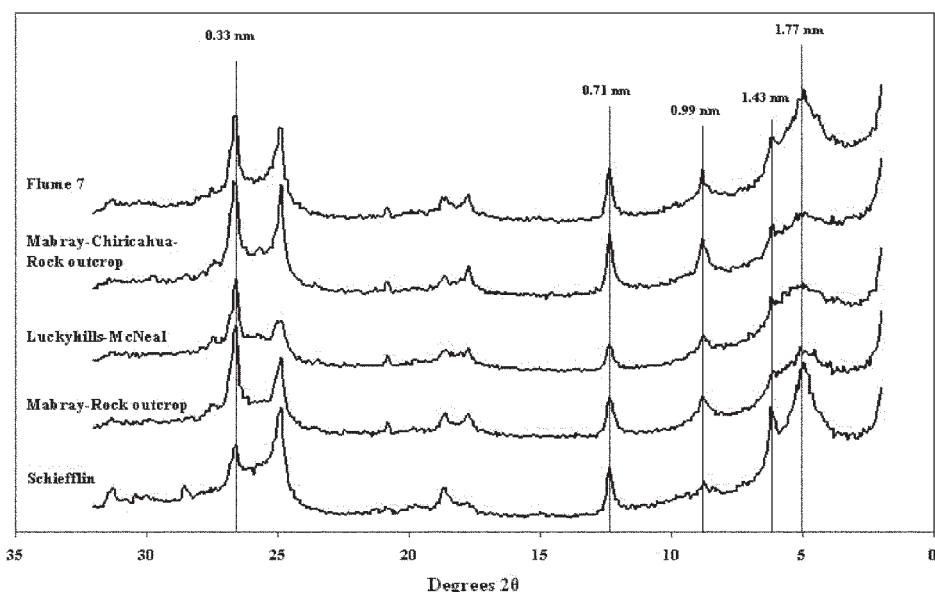

Fig. 4. Mineralogy of Mg-saturated, glycerol-solvated clays (<2 μm) from suspended sediments and selected watershed soils for Subwatershed 7.
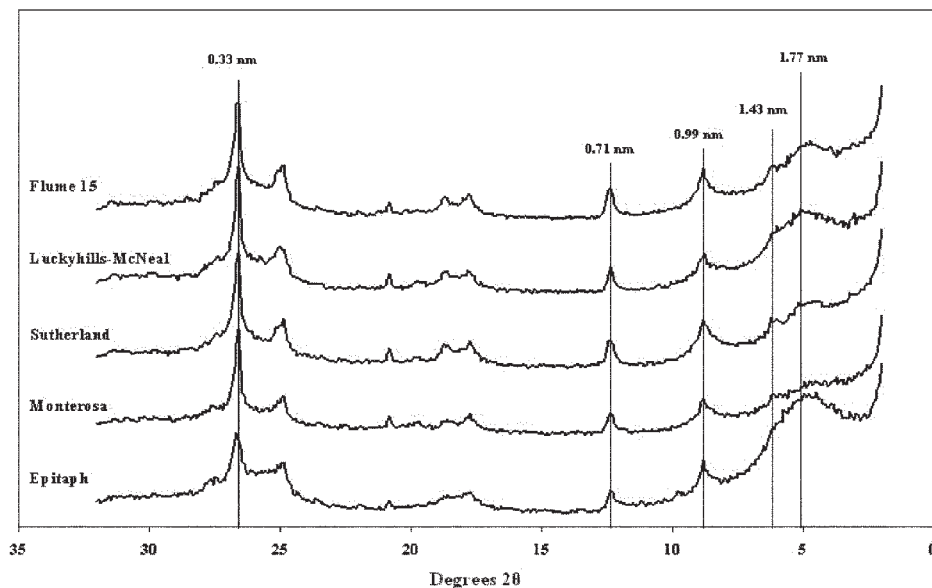
Fig. 5. Mineralogy of Mg-saturated, glycerol-solvated clays (<2 μm) from suspended sediments and selected watershed soils for Subwatershed 15.

Flume1. Since the parent materials, landforms, mapping units, and land-use in these unsampled portions of the watershed are essentially identical to the six SWs used in the study, it is reasonable to assume that the sediment entering the main channel from these areas is similar to that produced by identical soils in SWs 3, 7, 9, 10, 11, and 15. Furthermore, we can also assume that once the sediment from all SW sources is mixed over the length of the WGEW, our estimates of individual SW contributions are reasonably accurate.

The mean contribution of each SW to the sediment load monitored at Flume 1 and their associated standard deviations calculated from the multivariate mixing model results (Table 7) are as follows: SW 3, 46% (29); SW 7, 22% (30); SW 15, 18% (13.6); SW 10, 6% (4.4); SW 9, 4% (5.1); and SW 11, 4%
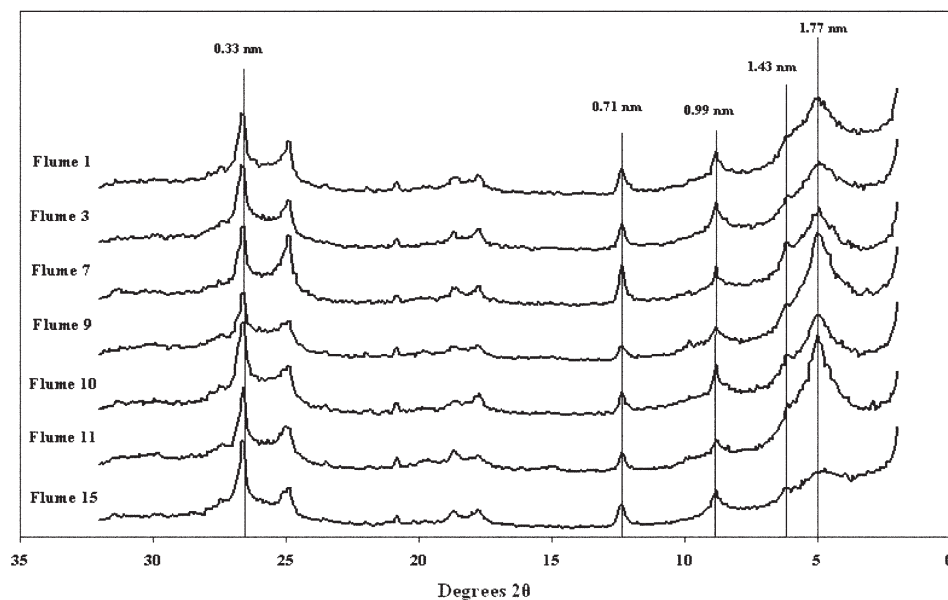

Fig. 6. Mineralogy of Mg-saturated, glycerol-solvated clays (<2 μm) from suspended sediments collected at Flumes 1, 3, 7, 9, 10, 11, and 15.

(7.4). The coefficients of variation (variability) are 29, 30, 76, 73, 128, and 185%, respectively. Generally, the SWs contributing the greatest amounts of sediment have the lowest coefficients of variation, which may be an indication that the SWs with the lower AI values (3 and 7) yield more consistently higher sediment loads at a wider range of rainfall intensities than those SWs with a higher AI value and greater soil aggregate stability.

Based on these data, approximately 86% of the suspended sediment leaving the WGEW originated in SWs 3, 7, and 15, and 14% from SWs 9, 10, and 11. The estimated low production from the latter three SWs may seem unrealistic; however, SW 11 is located the greatest distance from Flume 1 (Fig. 1) and is substantially smaller than the other SWs (Table 2). Although 345,260 m³ of total flow was measured at Flume 11 from 1999 to 2003, compared with approximately 155,650 m³ each at Flumes 3 and 7, only 4% of the sediment load at Flume 1 was attributed to SW 11. There are some factors that also support the estimates of source contributions from SWs 9 and 10. These SWs had two of the highest AI values, which means their soils were relatively unerodible as substantiated by their low clay ER. Thus, a greater percentage of their sediment is being transported in larger aggregate size fractions that settle out of the suspension closer to the source than some other SWs. This, coupled with their relatively long distance from Flume 1, may be a primary contributing factor to their relatively low estimated sediment contributions since SW 9 had the greatest area in the watershed with a total flow volume of 1,304,630 m³. Approximately 342,430 m³ of flow was measured at Flume 10 during this monitoring period, but at these greater distances from the watershed outlet there is much more opportunity for bank overflows, resulting in significant portions of the suspended sediment becoming entrained in floodplains adjacent to the streams, where it remains in the watershed above the outlet at Flume 1.

Relative to the three SWs (3, 7, 15) that contributed the greatest to the sediment load at Flume 1, the soils in SWs 3 and 7 had the lowest AI and the highest clay ER measured in the WGEW. These results correspond well with erosion results expected from highly erodible watersheds. Additionally, these two SWs are closest to the watershed

outlet at Flume 1. Thus, the sediment contributed by these SWs to the main channel is not subject to as much entrainment and does not undergo as much sorting before its delivery at Flume 1 compared with the other SWs. The estimated 18% contribution by SW 15 is surprising, considering its relatively long distance from Flume 1, and also because it had the second highest AI (i.e., lowest erodibility). The total flow at Flume 15 for 1999 to 2003 equaled 1,364,060 m³ or four to eight times greater than some of the other SWs. Thus, there is the potential for a greater proportion of the suspended sediment from SW 15, with its relatively high clay and finely divided C contents and shorter distance to Flume 1, to reach the watershed outlet than some other SWs due to the much larger flow volumes. Although SW 9 had flow volumes similar to SW 15, it also had the lowest clay ER (0.93) and a relatively low silt ER (2.29), indicating that a coarser sediment size distribution is being eroded from SW 9. When ^{137}Cs is removed from the mixing model, however, the estimated contributions from SW 15 drops from 18 to 2%. This raises a question as to the reliability of ^{137}Cs, but 62% (1490 ha) of SW 15 occurs on C class slopes or less (6–8%), making this the least sloping SW in the WGEW. Thus, a larger proportion of the erosion in SW 15 probably occurs as sheet erosion, which could transport greater amounts of ^{137}Cs, strongly sorbed to clay and organic matter at the soil surface, relative to rill or gully erosion, which erodes a greater proportion of subsurface materials containing substantially less ^{137}Cs.

The mixing model results were evaluated for goodness of fit using all 11 sediment properties (Table 8) by multiplying the decimal equivalent of the predicted contribution of the individual SWs to the total sediment load at Flume 1 by the value of each sediment property recorded at a given SW. The results for each sediment property were then summed across the six SWs to give a single predicted value to compare with the measured value for the same property at Flume 1. The data show an exceptionally close fit for most of the properties. The largest discrepancy appears to be the magnetic susceptibility values, which underpredicted the measured values at Flume 1 by approximately 12%. These results suggest that the estimated sediment contributions by the various SWs according to the mixing model are quite reasonable and seem to validate our assumptions that the sediment contributions of the three unsampled SWs did not adversely impact the data. Furthermore, the stable C isotope data (Table 5) indicate that 63.8% of the stable C isotopes in the suspended sediment passing Flume 1 is of C3 plant (shrubs) origin. At Flumes 3, 7, and 15, 68.1, 65.7, and 55.3% of the stable C isotopes are from C3 plants. The predominant vegetation on these three SWs is shrubs (whitethorn, creosote bush, tarbush, snakeweed, and burrowed). Various grass species (gramas, curly-mesquite, bush muhly, and tobosa) are prevalent in the other SWs. These data support the mixing model results, which indicate that SWs 3, 7, and 15 are contributing most of the suspended sediment leaving the WGEW at Flume 1 and also suggest a strong relationship between stable C isotope composition and the erodibility of these soils.

CONCLUSIONS

The results from this study indicated that three SWs (3, 7, and 15) produced an estimated 86% of the suspended sediment transported from the WGEW, and that the greatest sediment yields were recorded for SWs 3 (46%) and 7 (22%), which also had the most highly erodible soils. This demonstrates that an approach of characterizing watersheds on the basis of diagnostic watershed soil and suspended sediment properties in conjunction with digital elevation models, digitized soil surveys, and a mixing model has the potential to provide a reasonably accurate means of estimating which portions of a watershed are producing the greatest amounts of sediment. A considerable amount of additional research is necessary, however, to make this approach more comprehensive. The results from this approach do not allow estimates to be made relative to streambank vs. soil contributions. There is also a need to determine which soil mapping units are contributing the greatest amounts of sediment within individual SWs, especially from the standpoint of site-specific remediation. The accuracy of the multivariate mixing model used to calculate the relative contributions of subcomponents of the watershed to the total sediment load needs to be validated at a smaller scale than used in this research. Eventually, the ability to identify primary sediment sources in watersheds will contribute to a more efficient design of best management practices to affect maximum reductions in sediment and chemical contaminant loads in watersheds.

Table 7. Means and standard deviations (in parentheses) of the mixing model estimates for subwatersheds (SWs) 3, 7, 9, 10, 11, and 15 contributions to the suspended sediment load at Flume 1 in the Walnut Gulch Experimental Watershed for 1999 to 2003.

Sediment properties in model	Contribution to suspended sediment load					
	SW 3	SW 7	SW 9	SW 10	SW 11	SW 15
no.				%		
11	46 (13.5)	22 (6.5)	4 (5.1)	6 (4.4)	4 (7.4)	18 (13.6)

Table 8. Comparison of predicted vs. measured suspended sediment properties used in the mixing model.

Sediment property†	Predicted values by subwatershed (SW)						Sum of predicted values	Measured value at Flume 1
	SW 3	SW 7	SW 9	SW 10	SW 11	SW 15		
Magnetic susceptibility	47.8	49.7	6.8	7.4	6.3	20.7	138.7	156.8
Total N	0.81	0.39	0.05	0.08	0.06	0.28	1.67	1.69
Inorganic C	8.37	4.18	0.44	0.53	1.01	3.93	18.46	17.16
Fe_d	2.58	1.42	0.19	0.37	0.17	0.9	5.63	5.38
Mn_d	0.15	0.11	0.01	0.02	0.01	0.03	0.33	0.35
Fe_o	0.32	0.41	0.02	0.04	0.01	0.09	0.89	0.90
Mn_o	0.07	0.07	0.01	0.02	0.01	0.03	0.21	0.18
Fe_p	0.05	0.02	0.004	0.01	0.02	0.01	0.11	0.11
Mn_p	0.01	0.01	0.003	0.01	0.001	0.01	0.04	0.04
^{137}Cs	4.20	3.13	0.42	0.42	0.51	3.34	12.02	13.65
^{226}Ra	40.3	16.7	1.1	6.1	3.1	12.9	80.2	85.1

† Subscripts p, o, and d denote pyrophosphate-, oxalate-, and dithionite-extractable, respectively.

REFERENCES

Alonso, M.A. 1997. Controls on erosion, sub-basins of Walnut Gulch, Arizona. p. 861–866. *In* S. Wang et al. (ed.) Proc. Conf. on Management of Landscapes disturbed by Channel Incision, Oxford, MS. 19–23 May 1996. Ctr. for Computational Hydrosci. and Eng., Univ. of Mississippi, Oxford.

Ambrose, S.H., and N.E. Sikes. 1991. Soil carbon isotope evidence for Holocene habitat change in the Kenya Rift Valley. Science 253:1402–1405.

Bekele, A., and W.H. Hudnall. 2003. Stable carbon isotope study of the prairie–forest transition soil in Louisiana. Soil Sci. 168:783–792.

Bekesi, G., and J. McConchie. 1999. Groundwater recharge modelling using the Monte Carlo technique, Manawatu region, New Zealand. J. Hydrol. 224:137–148.

Biedenbender, S.H., M.P. McClaran, J. Quade, and M.A. Weltz. 2004. Landscape patterns of vegetation change indicated by soil carbon isotope composition. Geoderma 119:69–83.

Bonniwell, E.G., G. Matisoff, and P.J. Whiting. 1999. Determining the times and distances of particle transit in a mountain stream using fallout radionuclides. Geomorphology 27:75–92.

Boutton, T.W. 1996. Stable carbon isotopes of soil organic matter and their use as indicators of vegetation and climate change. p. 47–82. *In* T.W. Boutton and S. Yamasaki (ed.) Mass spectrometry of soil. Marcel Dekker, New York.

Boutton, T.W., S.R. Archer, A.J. Midwood, S.F. Zitzer, and R. Bol. 1998. δ^{13}C values of soil organic carbon and their use in documenting vegetation change in a savanna ecosystem. Geoderma 82:5–41.

Breckenfeld, D.J., W.A. Svetlik, and C.E. McGuire. 1995. Soil survey of Walnut Gulch Experimental Watershed. U.S. Gov. Print. Office, Washington, DC.

Caitcheon, C.G. 1998. The significance of various sediment magnetic mineral fractions for tracing sediment sources in Killimicat Creek. Catena 32:131–142.

Christensen, T., H. Ehdwall, and E. Stranden. 1990. Natural radiation, nuclear wastes and chemical pollutants. Nordic Liaison Committee for Atomic Energy, Stockholm.

Dearing, J.A., R.A. Morton, T.W. Price, and I.D.L. Foster. 1986. Tracing movements of topsoil by magnetic measurements: Two case studies. Phys. Earth Planet. Inter. 42:93–104.

Dibben, S.C., I.F. Jefferson, and I.J. Smalley. 1998. The "Loughborough loess" Monte Carlo model of soil structure. Comput. Geosci. 24:345–352.

Faulkner, B.R., W.G. Lyon, F.A. Khan, and S. Chattopadhyay. 2003. Modeling leaching of viruses by the Monte Carlo method. Water Res. 37:4719–4729.

Franzmeier, D.P., E.J. Pedersen, T.J. Longwell, J.G. Byrne, and C.K. Losche. 1969. Properties of some soils in the Cumberland Plateau as related to slope aspect and position. Soil Sci. Soc. Am. Proc. 33:755–761.

Gelderman, F.W. 1970. Soil survey: Walnut Gulch Experimental Watershed, Arizona. USDA-SCS Spec. Rep. U.S. Gov. Print. Office, Washington, DC.

Grimshaw, D.L., and J. Lewin. 1980. Source identification for suspended sediments. J. Hydrol. 47:151–162.

Harris, S. 1971. Index of structure: Evaluation of a modified method of determining aggregate stability. Geoderma 6:155–162.

Heimsath, A.M., J. Chappell, N.A. Spooner, and D.G. Questiaux. 2002. Creeping soil. Geology 30:111–114.

Honeycutt, C.W., R.D. Heil, and C.V. Cole. 1990. Climatic and topographic relations of three Great Plains soils: II. Carbon, nitrogen, and phosphorus. Soil Sci. Soc. Am. J. 54:476–483.

Ibrahim, N.M., A.H. Abd el Ghani, S.M. Shawsky, E.M. Ashraf, and M.A. Farouk. 1993. Measurement of radioactivity levels in soil in the Nile delta and Middle Egypt. Health Phys. 64: 620–627.

Klages, M.G., and Y.P. Hsieh. 1975. Suspended solids carried by the Gallatin River of southwestern Montana: II. Using mineralogy for inferring sources. J. Environ. Qual. 1:68–73.

McLean, E.O. 1982. Soil pH and lime requirement. p. 199–204. *In* A.L. Page et al. (ed.) Methods of soil analysis. Part 2. 2nd ed. Agron. Monogr. 9. ASA and SSSA, Madison, WI.

McPherson, G.R., T.W. Boutton, and A.J. Midwood. 1993. Stable carbon isotope analysis of soil organic matter illustrates vegetation change at the grassland/woodland boundary in southeastern Arizona, USA. Oecologia 93:95–101.

Neiheisel, J., and C.E. Weaver. 1967. Transport and deposition of clay minerals, southeastern United States. J. Sediment. Petrol. 37:1084–1116.

Nichols, M.H., K.G. Renard, and H.B. Osborn. 2000. Precipitation changes from 1956–1996 on the Walnut Gulch Experimental Watershed. J. Am. Water Resour. Assoc. 38:161–172.

NRCS. 1996. Soil survey laboratory methods manual. Soil Surv. Invest. Rep. 42. U.S. Gov. Print. Office, Washington, DC.

Oldfield, F., T.A. Rummery, R. Thompson, and D.E. Walling. 1979. Identification of suspended sediment sources by means of magnetic measurements: Some preliminary results. Water Resour. Res. 15:211–218.

Osborn, H.B., K.G. Renard, and J.R. Simanton. 1979. Dense networks to measure convective rainfall in the southwestern United States. Water Resour. Res. 15:1701–1711.

Peart, M.R., and D.E. Walling. 1988. Techniques for establishing suspended sediment sources in two drainage basins in Devon, UK: A comparative assessment. IAHS Publ. 174:269–279.

Pierson, F.B., and D.J. Mulla. 1990. Aggregate stability in the Palouse region of Washington: Effect of landscape position. Soil Sci. Soc. Am. J. 47:1407–1412.

Pimentel, D.P., C. Harvey, K. Resosudarmo, K. Sinclair, D. Kurz, McNair, S. Crist, L. Shpritz, L. Fitton, R. Saffouri, and R. Blair. 1995. Environmental and economic costs of soil erosion and conservation benefits. Science 267: 1117–1123.

Renard, K.G., L.J. Lane, J.R. Simanton, W.E. Emmerich, J.J. Stone, M.A. Weltz, D.C. Goodrich, and D.S. Yakowitz. 1993. Agricultural impacts in an arid environment: Walnut Gulch studies. Hydrol. Sci. Technol. 9:145–190.

Rhoton, F.E., W.E. Emmerich, D.C. Goodrich, S.N. Miller, and D.S. McChesney. 2006. Soil geomorphological characteristics of a semiarid watershed: Influence on carbon distribution and transport. Soil Sci. Soc. Am. J. 70:1532–1540.

Rhoton, F.E., W.E. Emmerich, D.C. Goodrich, S.N. Miller, and D.S. McChesney. 2007. An aggregation/erodibility index for soils in a semiarid watershed, southeastern Arizona. Soil Sci. Soc. Am. J. 71:984–992.

Rhoton, F.E., N.E. Smeck, and L.P. Wilding. 1979. Preferential clay mineral erosion from watersheds in the Maumee River basin. J. Environ. Qual. 8:547–550.

Ritchie, J.C., E.E. Clebsch, and W.K. Rudolph. 1970. Distribution of fallout and natural gamma radionuclides in litter, humus, and surface mineral soils under natural vegetation in the Great Smoky Mountains, North Carolina–Tennessee. Health Phys. 18:479–491.

Ritchie, J.C., and J.R. McHenry. 1990. Application of radioactive fallout cesium-137 for measuring soil erosion and sediment accumulation rates and patterns: A review. J. Environ. Qual. 19:215–233.

Ritchie, J.C., J.R. McHenry, and A.C. Gill. 1972. The distribution of ^{137}Cs in the upper 10 cm of soil under different cover types in northern Mississippi. Health Phys. 22:197–198.

SAS Institute. 1999. The SAS system for windows. SAS Inst., Cary, NC.

Schoeneberger, P.J., D.A. Wysocki, E.C. Benham, and W.D. Broderson. 2002. Field book for describing and sampling soils. Version 2.0. Natl. Soil Surv. Ctr., Lincoln, NE.

Simanton, J.R., K.G. Renard, C.M. Christiansen, and L.J. Lane. 1994. Spatial distributions of rock fragments along catenas in semiarid Arizona and Nevada, USA. Catena 23:29–42.

Simanton, J.R., and T.J. Toy. 1994. The relation between surface rock-fragment cover and semiarid hillslope profile morphology. Catena 23:213–225.

Slattery, M.C., T.P. Hurt, and J. Walden. 1995. The application of mineral magnetic measurements to quantify within-storm variations in suspended sediment sources. IAHS Publ. 229:143–151.

Sutherland, R.A., and R.B. Bryan. 1989. Variability of particle size characteristic of sheetwash sediments and fluvial suspended sediment in a small semiarid catchment, Kenya. Catena 16:189–204.

Wall, G.J., and L.P. Wilding. 1976. Mineralogy and related parameters of fluvial suspended sediments in northwestern Ohio. J. Environ. Qual. 5:168–173.

Wallbrink, P.J., A.S. Murray, and J.M. Olley. 1999. Relating suspended sediment to its original soil depth using fallout radionuclides. Soil Sci. Soc. Am. J. 63:369–378.

Walling, D.E. 2005. Tracing suspended sediment sources in catchments and river systems. Sci. Total Environ. 344:159–184.

Walling, D.E., and J.C. Woodward. 1992. Use of radiometric fingerprints to derive information on suspended sediment source. IAHS Publ. 215:153–164.

Whiting, P.J., G. Matisoff, W.F. Fornes, and F.M. Soster. 2005. Suspended sediment sources and transport distances in the Yellowstone basin. Geol. Soc. Am. Bull. 117:515–529.

Wilson, J.W., C.J. Mertens, P. Goldhagen, W. Friedberg, G. De Angelis, J.M. Clem, K. Copeland, and H.B. Bidasaria. 2005. Atmospheric ionizing radiation and human exposure. NASA Ctr. for Aerospace Inf., Hanover, MD.

Young, F.J., and R.D. Hammer. 2000. Soil–landform relationships on a loess-mantled upland landscape in Missouri. Soil Sci. Soc. Am. J. 64:1443–1454.